Rapidly re-computable EEG forward models for realistic head shapes

J.J. Ermer[1], J.C. Mosher[2], S. Baillet[1,3], and R.M. Leahy[1]

[1]*Signal & Image Processing Institute, University of Southern California, Los Angeles, CA USA*
[2]*Los Alamos National Laboratory, Los Alamos, NM USA*
[3]*Laboratoire de Neurosciences Cognitives & Imagerie Cerebrale, Hopital de la Salpetriere, Paris, France*

1. Introduction

Solution of the EEG source localization or inverse problem using model-based methods typically requires a significant number of forward model evaluations. Subspace-based inverse methods such as MUSIC [6] can require evaluation of the forward model at thousands of possible source locations. Techniques based on least-squares minimization may require even more.

The observed set of measurements over an M-sensor array is often expressed as a linear forward spatio-temporal model of the form:

$$\boldsymbol{F} = \boldsymbol{G}\boldsymbol{Q} + \boldsymbol{N} \qquad (1)$$

where the observed forward field $\boldsymbol{F}$ (M-sensors x N-time samples) can be expressed in terms of the forward model $\boldsymbol{G}$, a set of dipole moments $\boldsymbol{Q}$ ($3P$-dipoles x N-time samples) and additive noise $\boldsymbol{N}$.

Because of their simplicity, ease of computation, and relatively good accuracy, multi-layer spherical models [1], [7], have traditionally been used for approximating the human head; however, the spherical model does have several key drawbacks. By its very shape, the spherical model distorts the true distribution of passive currents in the brain, skull and scalp. Spherical models also require that the sensor positions be projected onto the fitted sphere (Fig. 1) resulting in a distortion of the true sensor-dipole spatial geometry and ultimately the computed surface potential. The use of a single best-fitting multilayer sphere has the added drawback of incomplete coverage of the inner skull region, often ignoring areas such as the frontal cortex. In practice, this problem is typically resolved by fitting additional spheres to those regions not covered by the primary sphere. The use of these additional spheres results in added complication in the forward model.

Using high-resolution spatial information obtained via X-ray CT or MR imaging, we can generate a more realistic head model. We represent the head as a set of contiguous regions bounded by surface tessellations of the scalp, outer skull, and inner skull boundaries. Since accurate *in vivo* determination of internal conductivities is not currently possible, we assume that the conductivities are homogeneous and isotropic within each region.

With the exception of simple geometries (e.g. spheres, ellipsoids), analytical solutions for the potentials over multilayer surfaces do not exist. For a surface of arbitrary shape, the surface potential can be found using the Boundary Element Method (BEM) or similar numerical techniques (cf. [5]) to solve the surface integral equation:

$$\sigma_0 v_\infty(\boldsymbol{r}) = \frac{(\sigma_j^- + \sigma_j^+)}{2} v(\boldsymbol{r}) + \frac{1}{4\pi} \sum_{i=1}^{m} (\sigma_i^- - \sigma_i^+) \int_{S_i} \left(v(\boldsymbol{r}') \boldsymbol{n}_i(\boldsymbol{r}') \cdot \frac{\boldsymbol{r} - \boldsymbol{r}'}{\|\boldsymbol{r} - \boldsymbol{r}'\|^3} \right) d\boldsymbol{r}' \quad , \boldsymbol{r} \in S_j \qquad (2)$$

The major drawback of BEM, and other numerical techniques is their computational cost, which can exceed that of multilayer sphere models by two to three orders of magnitude. This computationl burden limits the practical application of BEM in solving the EEG source localization problem. Lack of computationally efficient EEG forward modeling solutions for non-spherical surfaces appears to be the major barrier to widespread adaptation of these more realistic head models.

Past work in the area of efficient EEG forward models has primarily focused on multilayer spherical models, most notably [1], [2], and [7]. For realistic head models, Huang et al. [3] present a sensor-fitted sphere method for MEG whose accuracy approaches that of BEM, with a computational cost on the order of a multilayer sphere. A survey of several BEM solutions and methods for minimizing run-time computations is presented in [5].

Here we describe a straightforward method that allows for rapid evaluation of the EEG forward model over a realistic head shape. We show that the quality of the forward modeling solution approaches that of BEM, with recomputation time about 30 times faster than that of a multilayer spherical model. The proposed methodology has the added benefit of providing whole-head coverage.

2. Methods

In this study, we focused on two candidate methodologies: 1) adaptation of the MEG sensor-fitted sphere methodology described by Huang et al. [3] to EEG; 2) calculation of the forward-field at an arbi-

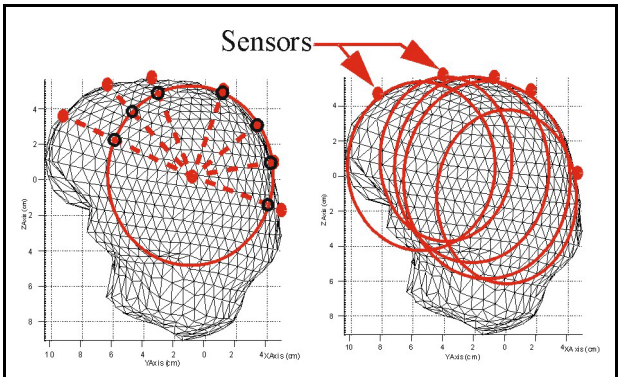

Figure 1: *(Left) Spatial distortion of true sensor positions (●) due to radial projection onto best-fit single-sphere model (**O**). (Right) Schematic plot of sensor-weighted sphere model.*

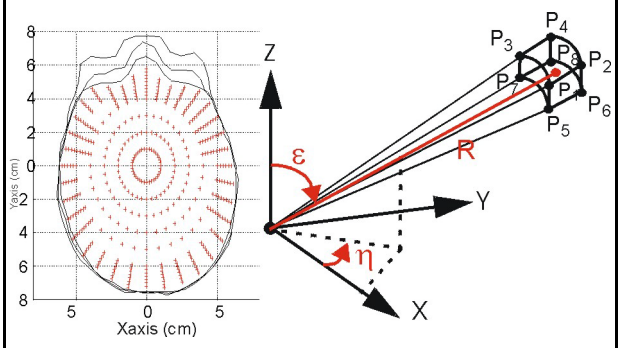

Figure 2: *(Left) Spherical grid points shown at level Z=0. (Right) Forward field interpolation based on weighted sum of 8 nearest grid points.*

trary dipole position via three-dimensional interpolation of the forward field over a pre-computed grid.

2.1. Sensor-fitted sphere

A schematic diagram of the sensor-fitted sphere model described in [3] is shown in Fig. 1. The objective of this method is to determine the center and radius of the fitted multilayer sphere which best approximates the true lead field for each individual sensor.

We first compute the lead field for each sensor using the linear Galerkin BEM form [5] over a representative grid of dipoles. Assuming fixed conductivity values and proportional sphere radii, we find the center $\boldsymbol{C}_0$ and outer radii R_0 of the multilayer sphere for the mth sensor whose lead field minimizes the function

$$\{R_0, C_0\} = \arg min(\left|\boldsymbol{g}_{sph}(\boldsymbol{r}, \underline{\boldsymbol{r}}', \underline{\sigma}, \underline{\rho} R_0) - \boldsymbol{g}_{BEM}(\boldsymbol{r}, \underline{\boldsymbol{r}}', \underline{\sigma})\right|) \quad (3)$$

The EEG sensor-fitted sphere model is then expressed as:

$$\boldsymbol{G}_{OS} = \begin{bmatrix} \boldsymbol{g}_{sph}(\boldsymbol{r}_1, \underline{\boldsymbol{r}}', \underline{\sigma}, \underline{\rho} R_0(1)) \\ \dots \\ \boldsymbol{g}_{sph}(\boldsymbol{r}_M, \underline{\boldsymbol{r}}', \underline{\sigma}, \underline{\rho} R_0(M)) \end{bmatrix} \quad (4)$$

2.2. Three-dimensional forward field interpolation

The three-dimensional forward field interpolation method is illustrated in Fig. 2. We define a set of grid points sampled in spherical coordinates (η,ε,R) throughout the inner-skull cavity. In our study, both azimuth η and elevation ε were sampled at 10^o intervals. We sampled along the radial direction at intervals of 2 mm when within 1-2 cm of the inner skull boundary and at 1 cm intervals elsewhere. We used the finer radial sampling in the vicinity of the surface boundary to account for the increased sensitivity of the forward field to variations in source locations within this region.

During the pre-computation phase, we use a BEM method to compute the (M x 3) forward field at each grid position. We then store this result as an indexed table for use by the interpolator during the inverse procedure. In our studies we compared two different BEM methods, "constant Galerkin" and "linear Galerkin," as reviewed by Mosher et al. [5].

At run-time, we determine the EEG forward model at an arbitrary location via three-dimensional trilinear interpolation of the forward-field solution corresponding to the eight nearest grid points (Fig. 2).

3. Results

We used the following metrics to evaluate pair-wise forward-field scale and subspace errors between the true forward gain matrix $\boldsymbol{G}_A$ and our approximation $\boldsymbol{G}_B$. We denote the (M-sensor x 1) forward field gain vector for the nth elemental dipole as $\boldsymbol{g}_A(n)$, where the $n=1,...,3P$ elemental dipoles correspond to the x, y, and z Cartesian components for each of the P dipoles.

Pairwise Forward Field PVU ($0 \le PVU \le 1$): The purpose of this metric is to evaluate scale error which serves as a predictor of forward model performance when using least-squares based approaches.

$$PVU(n) = \frac{\left|\boldsymbol{g}_B(n) - \boldsymbol{g}_A(n)\right|^2_{Fro}}{\left|\boldsymbol{g}_A(n)\right|^2_{Fro}} \qquad n = 1, \dots, 3P \quad (5)$$

Pairwise Forward Field Subspace Correlation: The purpose of this metric is to evaluate subspace error which serves as a predictor of forward model performance when using subspace-based approaches.

$$SBC_{FF}(n) = subcorr(\boldsymbol{g}_A(n), \boldsymbol{g}_B(n)) \quad n = 1, \dots, 3P \quad (6)$$

where *subcorr*(***a***,***b***) represents the cosine of the principle angle between the vectors ***a*** and ***b***.

3.1. Spherical model comparisons

To evaluate the impact of linear interpolation on EEG forward modeling error, we conducted a simple experiment using a three-layer sphere of increasing radii 8.1, 8.5, 8.8 cm with conductivities 0.33, 0.0042, 0.33 mhos respectively. A three-dimensional interpolative grid was set up using the sampling density described in Section 2.2.

We generated a set of dipoles falling at the center of each voxel (see Fig. 2). Dipoles within 3 mm of the inner layer boundary were included to simulate gyral cortical sources. The true forward model for each dipole was computed using an analytical multilayer sphere model. We then evaluated the interpolated solution performance using the *PVU* and *subcorr* metrics described in section 3.0.

While not shown here, we found that pairwise scale and subspace errors were extremely small ($PVU < 0.01$ and $subcorr > 0.99$) for all elemental dipoles. Our conclusion is that linear interpolation of the forward-field over a reasonably dense grid in the spherical model imposes little distortion with respect to the true solution.

3.2. Phantom model comparisons

We next tested the approach with a more realistic head shape. We used surface data from the human skull phantom described in Leahy et al. [4]. Using X-ray CT data, three surfaces (inner skull, outer skull, scalp) were tessellated to a density of 1016 triangles per layer. A representative set of 1,622 test dipole locations (4,866 elemental dipoles) were generated, where all dipoles were internal to both the inner skull and "best-fitted sphere" volumes. To evaluate model performance in gyral regions, we allowed dipole positions to fall within 3 mm of the inner skull boundary. The sensor array consisted of 54 sensors distributed approximately 3 cm uniformly over the upper portion of the phantom scalp. To establish a best estimate of EEG forward model "truth," we computed the linear Galerkin BEM solution for each test dipole. As shown in [5], the linear Galerkin method provides solutions with an effective PVU error of <0.01. Scale and subspace error metrics for each elemental dipole are shown in Fig. 3 for various forward models.

3.3. Computational & memory comparisons

Timing and memory metrics for various EEG forward modeling methods are shown in Table 1. All benchmarks were determined running MATLAB-based programs on a 500 MHz Pentium P-III PC with 512 MB RAM.

4. Discussion

With the increasing availability of surface extraction techniques for MRI and X-ray CT images, the major obstacle in widespread application of realistic EEG head models is the lack of a computationally efficient numerical procedure for computing the forward solution. Using multilayer sphere and realistic phantom experiments, we observed that three-dimensional interpolation of the EEG forward-field over a reasonably sampled grid produced highly accurate

Figure 3: *(Left) Pair-wise forward-field PVU (Left) and Pairwise forward-field subspace correlation (Right) between candidate forward model and Linear Galerkin BEM.*

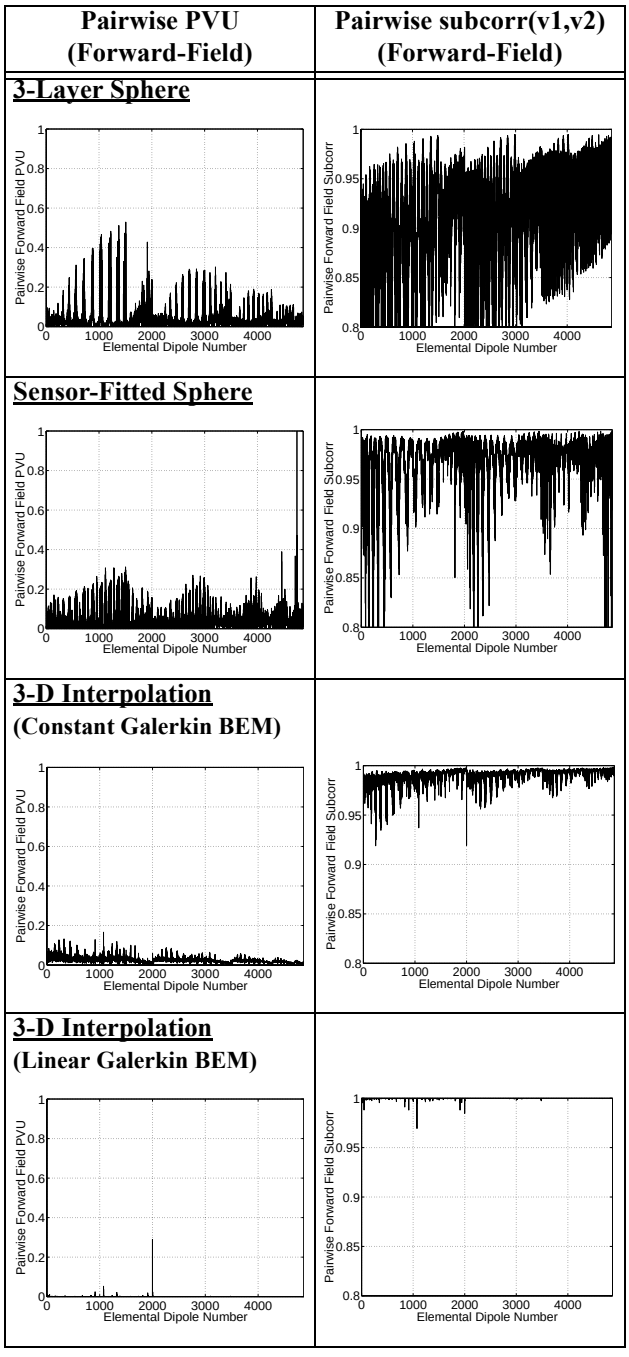

Table 1: *Computation and Memory Comparisons*

EEG Forward Model Method	One-Time Pre-Calculations (Sec)	Memory Storage (MB)	1622 Dipole Evaluation Time (Sec)
BEM (Constant Galerkin)	3,141.5	2.6	490.9
BEM (Linear Galerkin)	24,778.3	2.6	1,667.6
3-Layer Sphere N=100 Legendre	0.0	0.0	41.2
3-Layer Sphere Berg Approx.	34.2	0.0	2.36
Sensor Fitted Spheres	23,035.7	0.0	5.97
3-D Interpolation (Constant Galerkin BEM)	5,748.1	11.7	1.34
3-D Interpolation (Linear Galerkin BEM)	33,712.6	11.7	1.34

approximations to the true forward field. This accuracy was achieved even within 3 mm of the inner skull surface boundary. Exceptions were found only in extreme cases near rapidly changing surface boundaries (e.g. eye socket region) where the numerical solutions vary rapidly.

The spherical three-dimensional forward field interpolation is more than thirty times faster to compute than the traditional multilayer spherical forward model. We note that forward model recomputation time using the three-dimensional interpolation model is independent of the specific BEM method chosen. Cast in this framework, high fidelity numerical solutions currently viewed as computationally prohibitive for solving the inverse problem (e.g. linear Galerkin BEM [5]) can be rapidly recomputed in a highly efficient manner.

Both of the three-dimensional spherical interpolation models shown in Fig. 3 significantly outperform the multilayer sphere model in terms of subspace error and *PVU*. Constant and linear Galerkin BEM forms were observed to have subspace correlations better than 0.95 in nearly all cases. In comparison, the subspace correlations using a single best-fitted multilayer sphere often fell below 0.9. A reduction in *PVU* scale error was also observed. A somewhat less dramatic EEG forward modeling improvement was obtained using the fitted-sphere approach.

Realistic EEG forward models have the added advantage of being defined over the whole head. In comparison, the surface potential for a dipole located external to a locally-fitted sphere, yet still inside the skull, is undefined in a fitted sphere model.

Although the methods presented in this paper focus on the EEG forward model, the BEM interpolation method applies directly to MEG calculations with similar performance.

5. Acknowledgements

This work was supported in part by the National Institute of Mental Health under Grant ROI-MH53213, and in part by Los Alamos National Laboratory, operated by the University of California for the United States Department of Energy under Contract W-7405-ENG-36, and the Raytheon Doctoral Fellowship Program.

6. References

[1] P. Berg and M. Scherg, “A fast method for forward computation of multiple-shell spherical head models”, in Electroenceph. Clin. Neurophysiol, Vol. 90, 1994, pp. 58-64.

[2] J. de Munck, M. Peters, “A fast method to compute the potential in the multisphere model”, IEEE Trans. Biomed. Eng. Vol 40, 1993, pp. 1166-1174.

[3] M.X. Huang, et al., “A Sensor-Weighted Overlapping-Sphere Head Model and Exhaustive Head Model Comparison for MEG”, Phys. Med. Biol Vol. 44, 1999, pp. 423-440.

[4] R.M. Leahy et al., “A Study of Dipole Localization Accuracy for MEG and EEG using a Human Skull Phantom”, in Electroenceph. Clin. Neurophysiol, Vol. 107, 1998, pp. 159-173.

[5] J.C. Mosher, R.M. Leahy, and P.S. Lewis, “EEG and MEG: Forward Solutions for Inverse Methods”, in IEEE Trans. Biomed. Eng. Vol 46, March 1999, pp. 245-259.

[6] J.C. Mosher, P.S. Lewis, and R.M. Leahy, “Multiple Dipole Modeling and Localization from Spatio-Temporal MEG Data”, in IEEE Trans. Biomed. Eng. Vol 39, June 1992, pp. 541-557.

[7] Z. Zhang, “A Fast Method to Compute Surface Potentials Generated by Dipoles Within Multilayer Anisotropic Spheres”, Phys. Med. Biol Vol. 40, May 1995, pp. 335-349.